Introduction history and natural selection jointly shape evolution of a signaling trait during biological invasion

Jessica Pita-Aquino[1], Dan Bock[2], Simon Baeckens[3], Jonathan B. Losos[4], and Jason Kolbe[5]

[1]The University of Utah School of Medicine
[2]University of British Columbia
[3]Ghent University
[4]Washington University (WUSTL)
[5]University of Rhode Island College of Arts and Sciences

July 26, 2022

Abstract

Introductions of invasive species to new environments often result in rapid rates of trait evolution. While in some cases these evolutionary transitions are adaptive and driven by natural selection, they can also result from non-adaptive processes associated with the invasion history. Here, we examined the role of adaptive and non-adaptive evolutionary processes in the brown anole (Anolis sagrei), a widespread invasive lizard for which genetic data have helped trace the sources of non-native populations. We focused on the dewlap, a signaling trait known to be subject to multiple selective pressures. We measured dewlap reflectance, pattern, and size in non-native populations across the southeastern United States. We combine these trait measurements with quantification of environmental variables known to influence dewlap signal effectiveness, such as canopy openness. Further, we use genome-wide data to estimate ancestry and to perform association mapping for dewlap traits. We found that among-population variation in dewlap characteristics is best explained by ancestry, as contributed by invasion history. This result was supported by genome-wide association mapping, which identified several ancestry-specific loci associated with dewlap traits. Despite the strong imprint of invasion history on dewlap variation, we also detect significant relationships between dewlap traits and local environmental conditions. Thus, our results are also consistent with natural selection influencing trait evolution during the brown anole invasion. Our study clarifies the importance of ancestry and admixture in shaping phenotypes during biological invasion, while also showing that some traits can respond adaptively to conditions encountered in the invasive range despite potential constraints imposed by invasion history.

Introduction history and natural selection jointly shape evolution of a signaling trait during biological invasion

Running title

Dewlap evolution in non-native brown anoles

Authors

Jessica N. Pita-Aquino[a], Dan G. Bock[b], Simon Baeckens[c], Jonathan B. Losos[b], and Jason J. Kolbe[a]

Affiliation

[a]Department of Biological Sciences, University of Rhode Island, Kingston, RI 02881

[b]Department of Biology, Washington University in St. Louis, St. Louis, MO 63130

[c] Department of Organismic and Evolutionary Biology, Harvard University, Cambridge, MA 02138

Corresponding author

Jason J. Kolbe, jjkolbe@uri.edu

Present addresses:

Jessica N. Pita-Aquino: Department of Biochemistry, University of Utah School of Medicine, Salt Lake City, UT 84132

Dan G. Bock: Centre for Biodiversity Genomics, University of Guelph, Guelph, ON N1G 2W1, Canada
Simon Baeckens: Department of Biology, Ghent University, 9000 Gent, Belgium

Abstract

Introductions of invasive species to new environments often result in rapid rates of trait evolution. While in some cases these evolutionary transitions are adaptive and driven by natural selection, they can also result from non-adaptive processes associated with the invasion history. Here, we examined the role of adaptive and non-adaptive evolutionary processes in the brown anole (*Anolis sagrei*), a widespread invasive lizard for which genetic data have helped trace the sources of non-native populations. We focused on the dewlap, a signaling trait known to be subject to multiple selective pressures. We measured dewlap reflectance, pattern, and size in non-native populations across the southeastern United States. We combine these trait measurements with quantification of environmental variables known to influence dewlap signal effectiveness, such as canopy openness. Further, we use genome-wide data to estimate ancestry and to perform association mapping for dewlap traits. We found that among-population variation in dewlap characteristics is best explained by ancestry, as contributed by invasion history. This result was supported by genome-wide association mapping, which identified several ancestry-specific loci associated with dewlap traits. Despite the strong imprint of invasion history on dewlap variation, we also detect significant relationships between dewlap traits and local environmental conditions. Thus, our results are also consistent with natural selection influencing trait evolution during the

brown anole invasion. Our study clarifies the importance of ancestry and admixture in shaping phenotypes during biological invasion, while also showing that some traits can respond adaptively to conditions encountered in the invasive range despite potential constraints imposed by invasion history.

Keywords:

Anolis; genetic ancestry; invasive species; natural selection; invasion history; rapid evolution; dewlap

Introduction

Understanding how populations respond to environmental change is a key challenge in evolutionary biology. In recent decades, biological invasions have emerged as promising systems for studying evolution over contemporary time scales (Sakai et al., 2001; Sax et al., 2007). While representing imperfect experiments, invasions enable researchers to conduct studies at large spatial and temporal scales that would otherwise be impermissible for ethical reasons and to observe ecological and evolutionary processes in real time, which is often difficult with native-range populations (Sax et al., 2007; Lawson et al., 2011; Hodgins et al., 2018).

Rapid evolution during invasions can occur simultaneously through non-adaptive and adaptive processes. Of particular importance is the invasion history, which includes the contribution to genetic ancestry through the location and number of source populations in the native range (Kolbe et al., 2004, 2007a), the spread of populations in the non-native range (e.g., leading to 'expansion load'; Peischl et al., 2013), and the extent of admixture (i.e., intraspecific hybridization of previously isolated sources) within non-native populations (Rius & Darling, 2014; Bock et al., 2021). As a result of these processes occurring during an invasion, genetic and phenotypic variation can increase or decrease in invasive populations. For example, admixture will increase variation (Kolbe et al., 2004, 2008; Rius & Darling, 2014), whereas random genetic drift will decrease variation through founder effects and population bottlenecks (Dlugosch & Parker, 2008; Ficetola et al., 2008; Zhu et al., 2017). The invasion history is expected to leave a strong imprint on patterns of genetic and phenotypic variation within and among

77 non-native populations. When not properly accounted for, these non-adaptive
78 components of invasion history can strongly bias the interpretation of drivers of
79 evolution during invasions (Keller & Taylor, 2008; Colautti et al., 2009; Hodgins et al.,
80 2018).
81
82 Evolutionary trait change in invasive populations may also result from rapid adaptation
83 (Lee, 2002; Bock et al., 2015). Upon introduction, non-native populations often
84 encounter novel environments that differ in predators, competitors, and abiotic
85 conditions compared to their native-range source populations (Sakai et al., 2001).
86 These differences can release non-native populations from selective pressures
87 experienced in their native range and impose selection in new directions. Accordingly,
88 previous studies have demonstrated phenotypic shifts in non-native species driven by
89 natural selection (e.g., Huey et al., 2000; Colautti & Barrett, 2013; Bock et al., 2018),
90 which occurred rapidly over the course of tens to hundreds of generations (e.g., Huey et
91 al., 2000; Shine, 2011). Therefore, understanding evolution in introduced populations
92 will require elucidating the combined effects of invasion history and adaptation to
93 conditions encountered in the novel range.
94
95 The biological invasion of the brown anole lizard (*Anolis sagrei*) provides an excellent
96 opportunity to test alternative hypotheses for phenotypic evolution among non-native
97 populations. Native to the northern Caribbean—Cuba, Bahamas, Cayman Brac and
98 Little Cayman—the brown anole is a very successful invasive lizard that has been
99 repeatedly introduced to Florida (USA) and many other parts of the world. Multiple

introduction events from genetically distinct native-range populations have resulted in non-native populations with greater genetic diversity than those observed in the native range (Kolbe et al., 2007a, 2008; Bock et al., 2021). Also, non-native Florida populations are more morphologically variable in body size and shape, number of toepad lamellae and number of scales compared to native Cuban populations (Lee, 1992; Kolbe et al., 2007a). This increased phenotypic and genetic variation may promote evolution by natural selection, which could facilitate invasion success. Introduced populations differ significantly from each other in genetic variation and certain morphological traits (Kolbe et al., 2007a, 2008; Bock et al., 2021). At least eight introductions have occurred from different native-range sources into Florida (Kolbe et al., 2004) and as many as five sources contribute to a single non-native population (Kolbe et al., 2008). Thus, the invasion history may dominate patterns of phenotypic and genetic variation in these non-native populations. In such cases, the absence of strong natural selection or changes in the genetic architecture caused by genetic drift, admixture, and novel genetic interactions (e.g., Bock et al., 2021), may constrain adaptive responses.

By focusing on the brown anole across its invasive range, we examine adaptive and non-adaptive evolutionary change in the iconic *Anolis* signaling ornament: the dewlap. Dewlaps are extendable structures located on the throat of anoles that differ in size, shape, color, and patterning at both the inter- and intraspecific levels (Losos, 2009). This multifaceted signaling structure often plays an important role in territory establishment and defense (e.g., Fleishman, 1992), reproductive interactions (e.g.,

Crews, 1975), species recognition (e.g., Rand & Williams, 1970; Losos, 1985), and predator deterrence (e.g., Leal & Rodríguez-Robles, 1995; Leal & Rodríguez-Robles, 1997a,b). Considerable evidence supports that the dewlap is subject to a variety of selection pressures (Leal & Fleishman, 2002, 2004; Vanhooydonck et al., 2009; Ng et al., 2013a; Driessens et al., 2017).

Adaptive changes in signaling systems may occur in direct response to competitors, predators, or conspecifics (Cole, 2013), but may also arise to accommodate variation in climatic conditions and physical habitat characteristics (Endler, 1992, 1993). Indeed, previous research has shown strong, albeit contrasting, relationships between environmental conditions and dewlap design in native populations of *Anolis* lizards (Leal and Fleishman, 2002, 2004; Ng et al., 2013a; see Discussion for details). For brown anoles, Driessens et al. (2017) studied dewlap characteristics (i.e., color, pattern, and size) among populations distributed across its native range in the northern Caribbean. They reported that populations inhabiting mesic environments had primarily marginal dewlaps (i.e., red or orange covering most of the dewlap with yellow along the outer margin), showing high reflectance in red, whereas lizards occupying xeric environments had a higher proportion of solid dewlaps with higher UV reflectance. These results show that *Anolis* dewlap phenotypes are associated with variation in environmental conditions, likely resulting from differential selection on signal effectiveness.

In this study, we investigated dewlap color, pattern, and size in brown anole populations across a large portion of its non-native range in the southeastern United States. Our

goal was to determine whether among-population variation in aspects of dewlap design can be best explained by local adaptation, invasion history, or a combination of both factors. Specifically, we test whether variation in dewlap characteristics (i.e., color, pattern and size) are associated with 1) differences in prevailing environmental conditions (i.e., temperature, precipitation, and light conditions (Driessens et al., 2017) and 2) the relative genetic contributions from different native-range source populations (Kolbe et al., 2004, 2007a, 2008). We complement the latter ancestry-based tests with genome-wide association analyses, taking advantage of recent analytical developments that allow ancestry-specific associations to be detected along the genome (e.g., Skotte et al., 2019).

Materials and Methods

Study sites and sampling

We sampled 13-28 brown anoles from each of 30 populations in southeastern United States from Florida (*N* = 28 sites) and Georgia (*N* = 2 sites; Table S1). Sites were organized along three latitudinal transects (Figure S1), completed during three field trips in March-July 2018. Sampling was limited to natural habitats with variable understory light conditions and no evidence of artificial structures. However, we sampled two populations (i.e., LOW and TIF; Table S1) from landscaped vegetation and around hotel grounds due to low lizard densities. In all, we obtained 589 adult males, which were transported to the animal care facility of Harvard University. We kept the lizards for 5-9 weeks in the lab under uniform conditions in individual enclosures (see De Meyer et al., 2019 for a detailed enclosure description), during which time they were measured for a

range of related projects. Dewlap characteristics were scored for a subset of 570 lizards at 10-30 days after arrival from the field. All procedures described here for housing and measuring lizards were approved by the Harvard University Institutional Animal Care and Use Committee (IACUC protocol # 26-11).

Spectral data acquisition

Dewlap reflectance was measured with an Ocean Optics USB4000 spectrometer, a pulsed Xenon light source (PX-2, Ocean Optics), and a reflectance probe encased in a black anodized aluminum sheath. The reflectance probe was set at 45º to prevent specular reflection (i.e., glare; Endler, 1990). For each lizard, we collected reflectance data at three points: one in the center of the dewlap and two along the edge (Figure S2a). Dewlaps were extended using stainless-steel, reverse-action forceps. For each of the three points on the dewlap, we took three repeated measurements, resulting in nine measurements per individual. We calibrated the spectrometer after every three measurements using a Spectralon white and black standard and measured reflectance from 300 (ultraviolet, UV) to 700 nm (red) in 10-nm intervals (Cuthill et al., 1999). We included the UV spectral range since *Anolis* lizards have the capacity to perceive UV signals (Fleishman et al., 1993; Fleishman & Persons, 2001).

Spectral data processing

Spectrophotometric data were processed to reduce noise, remove technical artifacts, and analyze reflectance spectra using the package *pavo* (Maia et al., 2013) in R v.3.6.1 (R Development Core Team, 2011). Raw spectra were smoothed using the *procspec*

function, which applies the LOESS (Locally Weighted Scatterplot Smoothing) method with a quadratic regression and a Gaussian distribution. To normalize spectra and correct for negative values, we set the minimum value to zero and scaled up other values accordingly using the *procspec* function. We tested for repeatability of measurements taken at the same position on the dewlap using the R package *rptR* (Stoffel et al., 2017). Because all repeatability estimates were above 80%, we averaged repeated measurements using the *aggspec* function in *pavo*. We extracted three colorimetric variables: total brightness, cut-on wavelength, and UV reflectance. Total brightness was calculated as the area under the "uncorrected" spectral curve from 300 to 700 nm. To determine the UV reflectance and cut-on wavelength, the latter being a proxy for hue (i.e., the midpoint between baseline and maximum reflectance; Cummings, 2007), we corrected the spectra for brightness by making the area under each curve equal to 1.0 (Endler, 1990). This correction allows for identification of differences in spectral shape that are unrelated to brightness (Ng et al., 2013a).

Dewlap pattern

Each extended dewlap was photographed using a Nikon D3300 (24.2 MP) digital camera on a white background under standardized room lighting conditions in the lab. We included a color standard (i.e., X-rite Mini ColorChecker® Classic) and a ruler for scale. Images were calibrated using the *colorChecker* function in the R package *patternize* (Van Belleghem et al., 2018). This function calculates a second order polynomial regression between the observed and expected RGB (red, green, and blue) values and performs the calibration of the image.

To quantify the proportion of each color present in a given pattern, we determined the RGB values of the colors present in each pixel (size ≈ 0.007 mm) of the dewlap image using Color Inspector 3D (Barthel, 2006), a plugin for ImageJ (Rasband, 2012). This plugin displays the distribution of colors of an image within a 3D color space. We extracted the RGB values and their frequency and imported them to R. We obtained a list of known colors with their respective RGB values using the base R functions *colors* and *col2rgb*. Then, we classified dewlap RGB values for each pixel to color categories using Euclidean distance, which determines the nearest known color in RGB-space. Color composition was calculated as the percent of red, orange, and yellow present in each dewlap.

Brown anole dewlaps vary from a single color to some combination of red, orange, and yellow-colored patches. We categorized dewlap patterns into two types. 'Solid' dewlaps are uniformly colored and may contain a distinct marginal color, such as a reddish color covering most of the dewlap with a yellowish color along the outer margin (Figure S2b). 'Spotted' dewlaps have yellowish spots scattered across the reddish center and may also contain a yellow outer margin (Figure S2c).

Dewlap size

We measured dewlap area and perimeter from digital photos in ImageJ. Dewlap area and perimeter were measured by creating line segments throughout the border of the dewlap, ultimately forming a polygon and obtaining the area and perimeter of it. We

measured the dewlap for each lizard twice to verify the repeatability of this method, which was 1.0. We used a digital x-ray system to capture skeletal images from euthanized lizards. Using ObjectJ, a plug-in for ImageJ, we estimated of body size by measuring snout-vent length (SVL), the distance from the tip of the snout (i.e., the edge of the soft tissue) to the final vertebrae that had forward-facing arms. SVL values were then log-transformed and regressed against log-transformed dewlap area and perimeter. The resulting residual values represent body size-corrected dewlap size.

Environmental data

To estimate the amount of light filtered through the forest canopy, we took hemispherical photos with a 180º fisheye lens at the location where each lizard was first observed. Canopy photos were analyzed in Hemispherical_2.0, a macro for ImageJ, which calculates the percentage of pixels that are open sky (Beckschäfer, 2015).

We characterized environmental variation using Geographic Information System (GIS) climate layers interpolated from average monthly climate data from weather stations with a spatial resolution of about 1 km^2 (WorldClim database; Hijmans et al., 2005). For each sampled locality, we extracted two bioclimatic variables that have been considered important for explaining dewlap color variation in anoles: annual precipitation and annual mean temperature (Williams, 1974; Ng et al., 2013a; Driessens et al., 2017).

Statistical analyses

Reflectance spectra can be interpreted as a multivariate phenotype, where reflectance values at each discrete wavelength are a variable. Therefore, dewlap color can be represented in a multidimensional color space. To reduce the dimensionality of the spectral data, we binned reflectance values into 10-nm bins using the *procspec* function in *pavo* (Maia et al., 2013). Each of the three positions on the dewlap where we took spectral readings was included as a separate variable and repeated measurements at each position were averaged. We used the base R function *prcomp* to conduct a principal component analysis (PCA) on 123 variables representing the reflectance spectra.

We conducted linear mixed effect models using *lme4*, *lmer* and *lmerTest* packages in R (Bates et al., 2015; Kuznetsova et al., 2017). For these models, we assigned principal component (PC) axes 1 or 2, which includes all colorimetric variables across the spectral range, as the response variables. Further, percent Western Cuban ancestry (see 'Population structure and genetic diversity' section below) was included as a fixed factor along with the covariates annual mean temperature, annual mean precipitation, and canopy openness. We also included site as a random effect to account for variation among populations not related to our main hypotheses. To further investigate dewlap variation, we used models with the same covariates, as well as fixed and random effects as previously described to evaluate individual variables describing aspects of the dewlap: UV reflectance, total brightness, and hue across the three dewlap positions; color composition of red, orange, and yellow; and dewlap size (i.e., area and perimeter). We log-transformed data to improve normality when appropriate.

We performed a generalized linear model, specifically a binomial logistic regression, to identify whether any variables predict dewlap pattern (i.e., solid or spotted) using the base R function *glm*. The predictor variables were Western Cuban ancestry, canopy openness, annual mean temperature, and annual mean precipitation. All statistical analyses were performed in R.

Genome-wide SNP genotyping

We used the same samples and quality-filtered reads included in our previous study on the genetic architecture of limb length in *A. sagrei* (Bock et al., 2021). This sampling includes the *A. sagrei* males used here for dewlap measurements, non-native population samples obtained earlier in the invasion (i.e., in 2003), and samples from the native range of *A. sagrei*. Using quality-filtered reads for all samples (see detailed methods in Bock et al., 2021), we repeated the SNP calling and variant filtering steps based on version 2.1 of the *A. sagrei* genome, which recently became available (Geneva et al., 2021). Reads were aligned to the genome using the dDocent v2.2.20 pipeline (Puritz et al., 2014), and SNPs were called using Freebayes v. 1.3.2 (Garrison & Marth, 2012).

Filtering of the resultant variant calls was implemented using vcflib (https://github.com/vcflib/vcflib) and consisted of sequential steps based on number of alleles (i.e., keeping only biallelic markers), type of variant (i.e., keeping only SNPs), read mapping quality (i.e., using SNPs with a MAPQ score > 20), and depth of

sequencing (i.e., keeping only genotypes with DP > 3). For the remaining filtered SNPs, we used BCFtools v.1.9 (Narasimhan et al., 2016) to subset genotypes corresponding to the sequenced *A. sagrei* individuals obtained in 2018 from Florida and Georgia, for which dewlap trait data was also available (N = 560). We then kept only SNPs with data at more than 70% of these samples and only SNPs with a minor allele frequency > 1%. Of the resulting 120,623 SNPs, we removed candidate gametolog SNPs following Bock et al., (2021). These gametolog SNPs occur on the X chromosome of *A. sagrei* (Geneva et al., 2021) and are a result of homology between the X chromosome (i.e., scaffold 7 in the *A. sagrei* v2.1 genome assembly) and the Y chromosome, which is currently not included in the genome assembly. After gametolog removal, the final filtered SNP set contained 120,387 SNPs.

Population structure and genetic diversity

To summarize population structure, we relied on 10,000 random SNPs, obtained from the filtered SNP set using the "vcfrandomsample" option in *vcflib*. We then used Bayesian clustering as implemented in STRUCTURE v.2.3.4 (Pritchard et al., 2000). We considered K values from 1 to 10. For each K value, we used 20 independent replicates. Each replicate used the first 150,000 iterations as burn-in, followed 150,000 MCMC repetitions. We then used the *pophelper* (v.2.3.0; Francis, 2017) R package to estimate the most likely number of clusters in our data based on the delta K method (Evanno et al., 2005) and to plot the STRUCTURE results. We supplemented these analyses with a discriminant analysis of principal components (DAPC) performed using the *adegenet* R package (v. 2.1.1; Jombart & Ahmed, 2011). We further calculated

heterozygosity as the percent heterozygous SNPs out of all SNPs with data for a given individual. This approach partitions our dataset into two groups (K = 2) with predominantly Western Cuba ancestry and reduced heterozygosity (hereafter referred to as the "Western Cuba ancestry" group), and a group of mostly admixed individuals (higher genome-wide heterozygosity; two-sided Wilcoxon rank-sum test, W = 9, P = 6.917 x 10^{-6}; see also Bock et al., 2021) with ancestry from Central and Eastern Cuba (hereafter referred to as the "Central-eastern Cuba ancestry" group). Because all samples included in our dataset are males, sex chromosome SNPs will not bias diversity estimates, as would happen if we had included both males and females. Therefore, heterozygosity estimates were based on all 10,000 random genome-wide SNPs, irrespective of their position along the genome.

Genome-wide association mapping for dewlap traits

The genome-wide association study (GWAS) was based on all filtered markers (120,387 SNPs). Prior to GWAS, missing data was imputed using BEAGLE v5.0 (Browning & Browning, 2016), at default settings. To investigate correlations among the 11 traits that capture dewlap size (i.e., area and perimeter) and color (i.e., hue, total brightness, mean brightness, UV chroma, red chroma, yellow chroma, and composition of red, orange, or yellow), we first used the *ggcorrplot* R package (v. 0.1.3; Kassambara, 2019). The GWAS was then performed using two complementary approaches, which we refer to as the "standard GWAS" and the "ancestry-specific GWAS". The standard GWAS consisted of a linear mixed model implemented in GEMMA (Zhou & Stephens, 2012) and included SNPs on the 10 largest chromosomes

(i.e., 117,301 SNPs or 97.4% or all filtered SNPs). We first used GEMMA to calculate 10 relatedness matrices, by excluding SNPs from one chromosome at a time (i.e., each matrix was based on SNPs from 9 chromosomes). The GWAS for markers on a given chromosome was then performed using the relatedness matrix that excluded markers on that same chromosome. This approach should improve power to detect associations, given that the relatedness matrix does not include markers that are in linkage disequilibrium with the marker being tested (Cheng et al., 2013). We then obtained *P* values from the Wald test as outputted by GEMMA.

The ancestry-specific GWAS was conducted in asaMap (Skotte et al., 2019), and included SNPs on the 50 largest chromosomes in the assembly (i.e., 120,232 SNPs or 99.9% of all filtered markers). We used only these chromosomes to facilitate data conversion from VCF to the PLINK binary biallelic genotype table (i.e., ".bed" format) used by asaMap. The conversion from VCF to .bed files was done in PLINK v1.9 (Purcell et al., 2007). To control for the confounding effect of population structure during GWAS, we used the first 10 PCs from a PCA computed using the *adegenet* R package (v. 2.1.1; Jombart & Ahmed, 2011). These 10 PCs were included as covariates in the asaMap analysis. The PCA was based on 10,000 random SNPs, obtained from the complete SNP set. The asaMap software performs eight association tests, with and without different ancestry-specific effects considered for two ancestral populations (Skotte et al., 2019). Following asaMap manual recommendations, we estimated genome-wide ancestry proportions of each sample, as well as SNP allele frequencies for each ancestral population using ADMIXTURE v. 1.3.0 (Alexander et al., 2009). For

each dewlap trait, we obtained genome-wide *P* values for all tests and selected the test with the strongest association (i.e., the lowest observed *P* value among all tested SNPs), following Bock et al., (2021).

For both the standard and the ancestry-specific GWAS results, we used the *GenABEL* R package (Aulchenko et al., 2007) to calculate the lambda genomic inflation factor (λ), and account for any remaining *P* value inflation, which can be caused by unaccounted population stratification. Genome-wide significance thresholds were then set using the conservative Bonferroni method (0.05/total SNPs used for the association test). We also considered a suggestive genome-wide significance threshold (1/total SNPs used for the association test; Duggal et al., 2008), for which one false positive per GWAS is expected. To visualize GWAS results, we used Manhattan and quantile-quantile (QQ) plots, made in R v.4.1.0 using publicly available scripts (Manhattan: https://danielroelfs.com/blog/how-i-create-manhattan-plots-using-ggplot/; QQ: https://genome.sph.umich.edu/wiki/Code_Sample:_Generating_QQ_Plots_in_R). Finally, to estimate the effect size of associations that were significant at either of the two genome-wide thresholds, we build linear models in R. These models had number of alternative alleles (i.e., alleles different from those incorporated in the reference genome) at the lead GWA SNP as the predictor variable, and the corresponding dewlap trait as the response variable. Effect sizes were then estimated as R^2 values, using the "summary" function in R.

To better understand the observed effect of ancestry on dewlap traits, we next focused on results of the ancestry-specific GWAS. Specifically, we investigated how dewlap traits vary among genotype classes, for ancestry-specific associations that passed the Bonferroni or suggestive significance thresholds. For this, we stratified the invasive *A. sagrei* samples based on ancestry, using a cutoff of 70% Western Cuba ancestry, as inferred using the STRUCTURE analysis. Because of the genetic makeup of invasive *A. sagrei* populations across the southeastern United States, this approach partitions samples into two groups, one with limited hybridization (i.e., Western Cuba ancestry samples) and another with frequent hybrids for which Central-eastern Cuba ancestry predominates (see also Bock et al. 2021).

Results

Dewlap characteristics

Dewlap reflectance spectra revealed consistent patterns across populations (Figure S3). Despite individual variation in spectral characteristics, most lizards showed peak reflectance values between 600 to 700 nm wavelengths (Figure 1a). The relative intensity of UV wavelengths (300 to 400 nm) varied across individuals; dewlaps with greater proportions of yellow had higher UV reflectance values.

When comparing PC axes, dewlap reflectance showed strong differentiation between red and yellow-dewlapped lizards (Figure 1b). PC1 explained 63.7% of the variation, whereas PC2 explained 15.6%. High values of PC1 corresponded to relatively bright

dewlaps, whereas low PC1 values corresponded to dull dewlaps. As for PC2, high values corresponded to red dewlaps and low values to yellow ones.

Population structure

The delta K criterion confirmed that two genetic clusters (K = 2) are the best fit for our data (Figure S4a-c). As expected, given results from our previous study on genomic variation in these populations (Bock et al., 2021), all individuals were assigned ancestry from both genetically distinct clusters in varying proportions. Based on information from mtDNA sequences (Kolbe et al., 2004, 2007a) and genome-wide SNP data from the native range (Bock et al., 2021), these clusters can be interpreted as representative of ancestry from native lineages in western and central-eastern Cuba. Southern Florida populations have higher frequencies of Western Cuba ancestry, whereas central to northwestern Florida populations are highly admixed, and contain higher frequencies of Central-eastern Cuba ancestry (Figure S5). Note, however, that DAPC indicated that a clustering of K = 3 could be a marginally better fit (Figures S7-S8).

Associations between the dewlap, ancestry, and the environment

We found significant correlations between dewlap traits, ancestry, and environmental variables. Dewlap variation as represented by PC1 and PC2 showed significant positive correlations with Western Cuban ancestry ($P < 0.001$, Table 1). As the frequency of Western Cuban ancestry increased, lizards exhibited brighter and redder dewlaps (Table 1, Figure 1, Figure S6a,b). Additionally, PC1 was negatively correlated with

canopy openness (P = 0.002; Table 1). As canopy openness increased (i.e., less canopy cover and lighter conditions), lizards exhibited darker dewlaps.

To further investigate the effects of ancestry and environmental conditions on distinct aspects of the dewlap, we built separate models for each dewlap trait including UV reflectance, total brightness, hue (cut-on wavelength), color composition (red, orange, yellow), area, and perimeter. Spectral colorimetric variables differed across dewlap positions; therefore, further analyses were also done by position (i.e., P1, P2 and P3). UV reflectance was negatively correlated with Western Cuban ancestry across dewlap positions (P1–edge, P = 0.003; P2–edge, P = 0.03; P3–center, P = 0.019; Table 1). Center UV reflectance showed significant positive correlations with canopy openness (P2, P < 0.001; P3, P = 0.02) and annual mean precipitation (P2, P = 0.033). Total brightness was positively correlated with Western Cuban ancestry (P2 and P3, P < 0.001) and negatively correlated with canopy openness (P1, P < 0.001; P2, P = 0.03). These univariate results are consistent with PC analyses, such that PC1 can be interpreted as brightness. Both PC1 (Figure S6a,k) and total brightness (Figure S6f,g,n,o) resulted in significant positive correlations with Western Cuban ancestry and negative correlations with canopy openness across dewlap positions (Table 1). PC2 and yellow composition were correlated with Western Cuban ancestry (P < 0.01; Figure S6); lizards with low PC2 values had yellow dewlaps (i.e., greater yellow composition) and low frequencies of Western Cuban ancestry. As for size, dewlap area and perimeter resulted in significant positive correlations with Western Cuban ancestry (Figure S6i-j) and negative correlations with canopy openness (Figure S6p-q; Table 1). The

464 colorimetric variable hue (cut-on wavelength) was inconclusive due to lack of model
465 convergence.
466
467 Binomial logistic regression indicated that the probability of a lizard having a solid
468 dewlap increased with Western Cuban ancestry (P = 0.01; Figure S9c). Although we
469 observed variation in dewlap pattern across populations (Figs. S9-S10), this trait was
470 not significantly correlated with any environmental variable (Table 2). Furthermore, we
471 found no significant correlation between red color composition, ancestry, and
472 environmental variables. However, yellow color composition was negatively correlated
473 with Western Cuban ancestry (P = 0.01, Figure S6h). These results are consistent with
474 analyses of PC2. Lizards with low PC2 values had yellow dewlaps (Figure 1b) and low
475 frequencies of Western Cuban ancestry (Figure S6b).
476
477 **Genetic architecture of dewlap traits**
478 Analysis of correlations among traits (Figure S11) revealed strong and significant
479 correlations between our measurements of dewlap size (i.e., area and perimeter; *r* =
480 0.91) and between our measurements of dewlap brightness (i.e., mean and total dewlap
481 brightness; *r* = 1). Moderate, albeit still significant, positive correlations were further
482 revealed between dewlap hue, yellow chroma, and brightness, as well as between
483 dewlap size and dewlap red chroma. Finally, dewlap UV chroma was negatively
484 correlated with most dewlap traits (Figure S11).
485

The linear mixed model implemented in GEMMA (i.e., standard GWAS), identified four loci distributed on macrochromosomes 4, 6, and 7 as significantly associated with the percent of red color (Figures 2, S12-S13). These associations were of moderate effect (percent variance explained 5.9 to 9.1%; Figure S13). All other analyses, including those based on the asaMap models (i.e., ancestry-specific GWAS) did not reveal any associations with dewlap traits at the Bonferroni-adjusted significance level (Figure S12). There were, however, SNPs that passed the suggestive genome-wide significance threshold using both GWAS approaches. These suggestive associations were identified for nine of the dewlap traits, and were distributed on macrochromosomes 1,2,4,5, and 6 (Figure 2, S12).

The ancestry-specific GWAS performed in asaMap indicated that, for dewlap UV chroma, the strongest genome-wide associations are those for models that assume an effect only in ancestral population 1, which corresponds to Central-Eastern Cuba ancestry (Table S2). Conversely, for dewlap brightness, ancestry-specific models indicated an effect only in ancestral population 2, which corresponds to Western Cuba ancestry. More detailed investigation confirmed that most of these SNPs (4 of 5 distinct SNPs) show an effect only in individuals that are part of the Western Cuba ancestry group (for dewlap brightness), or in those that are part of the Central-Eastern Cuba ancestry group (for dewlap UV chroma; Figure 3). For both dewlap brightness and dewlap UV chroma, ancestry-specific associations were of moderate effect, explaining 3.1% - 6.2% of trait variance (Figure 3).

Discussion

Our results show that dewlap variation in invasive brown anoles is primarily a result of non-adaptive evolution related to invasion history, with multiple aspects of dewlap coloration showing strong and significant correlations with genetic ancestry. GWAS results corroborated these findings and indicated that most dewlap traits have a complex genetic architecture. We identified four loci significantly associated with red coloration of dewlaps. For all other traits, however, loci were only suggestively associated with trait variation, occasionally with ancestry-specific effects. Our finding that invasion history in an important evolutionary force driving trait differentiation among non-native populations is consistent with previous studies of invasive species (e.g., *Silene vulgaris*, Keller & Taylor, 2010; sticklebacks, Lucek et al., 2010), including in the brown anole (Kolbe et al., 2007a). Even so, we find that multiple aspects of the dewlap are related to local environmental conditions, consistent with the role of natural selection. These findings support the hypothesis of adaptive signal divergence, which predicts that dewlap phenotype is correlated with environmental variation thus suggesting local adaptation (Leal & Fleishman, 2004). This study provides insight into the ongoing evolutionary processes occurring in invasions and highlights the importance of invasion history in phenotypic evolution, but not to the exclusion of adaptive processes.

Invasion history and its role in modulating dewlap phenotypes

Genetic clustering analyses revealed that ancestry of invasive brown anoles can be summarized at a coarse level as belonging to two genetically distinct native lineages:

Western Cuba and Central-eastern Cuba. Western Cuban ancestry was strongly correlated with several dewlap traits, including UV reflectance, brightness, coloration, size, and patterning. As the frequency of Western Cuban ancestry increased, lizards exhibited brighter and redder dewlaps with lower reflectance in UV (Table 1, Figure 1b, S6a-h). As well, the probability of lizards having a solid dewlap increased with the frequency of Western Cuban ancestry (Figure S9c). This result is consistent with findings from the native range which, while based on more limited sampling, also find that Western Cuban populations of *A. sagrei* have a greater proportion of solid dewlaps, whereas Central-eastern Cuban populations have a greater proportion of spotted dewlaps (Driessens et al., 2017). Therefore, these results point to an important role of invasion history and ancestry in shaping multiple dimensions of dewlap variation across invasive populations in this system.

In many organisms, carotenoid pigments have been shown to be a source of variation in red, orange, and yellow ornamental coloration within and between species (reviewed in Toews et al., 2017). In most animal species, carotenoids cannot be synthesized and must be ingested. The extent to which dewlap color variation is influenced by nutritional condition has so far been investigated in one anole species, *A. distichus* (Ng et al., 2013b). This study found no difference in color between carotenoid and control treatments and that dewlap coloration was heritable. Moreover, biochemical investigations of dewlap pigment composition in several *Anolis* species have found that pterin pigments are important sources of coloration, although carotenoids were detected as well (Ortiz, 1962; Macedonia et al., 2000, Steffen & McGraw, 2007, 2009). In

555 contrast to carotenoids, pterins are produced endogenously (reviewed in Andrade &
556 Carneiro, 2021). Even so, identifying genes involved in pterin synthesis has been
557 challenging because of the complexity of underlying biochemical pathways. For
558 example, studies contrasting skin patches of different color in other reptiles have
559 identified tens to hundreds of genes that are differentially expressed, and that are likely
560 involved in the production of these pigments (e.g., McLean et al., 2017). Our finding that
561 dewlap phenotypes are correlated with genome-wide estimates of ancestry across non-
562 native populations is in line with these previous studies and suggests a complex genetic
563 architecture for dewlap traits.
564
565 To better understand the effect of ancestry on dewlap variation, we used genome-wide
566 association analyses. We identified SNPs significantly associated with only one dewlap
567 trait (i.e., percentage of red color) at the Bonferroni-adjusted threshold (Figures 2, S13).
568 We note, however, that because of the elevated linkage disequilibrium (LD) that
569 characterizes these populations and non-independence of SNPs that are in LD (Bock et
570 al., 2021), the Bonferroni method used to determine this threshold may well be overly
571 conservative. At a more relaxed significance threshold, we detected associations for
572 nine of the 11 dewlap traits used for GWAS, distributed across macrochromosomes 1,
573 2, 4, 5, and 6.
574
575 We previously used the same samples to identify a large-effect locus significantly
576 associated with limb length in *A. sagrei* (Bock et al., 2021). Our results here indicate
577 that the genetic architecture of most dewlap traits is likely different and more complex

than that characterizing limb length, at least for *A. sagrei* of Cuban ancestry. This interpretation is further supported by among-trait correlations. While all limb length traits show strong and significant pairwise correlations (Bock et al., 2021), dewlap traits are characterized by more moderate among-trait correlations that are occasionally non-significant (Figure S11).

The associations identified here between SNPs and dewlap traits should be interpreted with caution for two reasons. First, aside from associations reported for red composition of the dewlap, the strength of the association signal is reduced for any one SNP. Second, in-depth analyses of standard and ancestry-specific associations (Figure 3 and Figure S13) revealed that genotype classes with the largest difference in trait values are also the ones with the lowest sample size (e.g., genotype GG for Western Cuba ancestry, at Chr2: 166.587 Mb; Figure 3). Therefore, some of these results could be due to uneven sample sizes among genotype classes. With these caveats in mind, we note that the direction of the ancestry-specific effects reported here is consistent with our observations of the effect of Western Cuba ancestry on dewlap trait variation. Specifically, linear mixed effects models of dewlap traits based on ancestry as well as the ancestry-specific GWAS indicated that Western Cuba ancestry is associated with increased brightness of dewlaps.

Adaptation to novel environments

We tested the hypothesis that dewlap phenotypes are correlated with environmental variation, which is expected under local adaptation. Supporting this prediction, we found

significant relationships between multiple environmental variables and dewlap characteristics. Our results show that dewlaps tend to be darker with relatively high UV reflectance as canopy openness (i.e., habitat light) increases. Also, we found that brown anoles occurring in habitats with greater precipitation had more UV reflectance. These findings are consistent with those obtained by previous studies in the native range of *A. sagrei*. Driessens et al. (2017) found that lizards occupying open forest habitats had higher UV reflectance than populations inhabiting environments with little light exposure.

Studies in other *Anolis* species show different correlations between UV reflectance and the environment, suggesting the relationship between aspects of the dewlap and the local environmental conditions might be species specific. For example, Ng et al. (2013a) found no difference in UV reflectance among *A. distichus* populations inhabiting environments that differed in light characteristics. Also, Leal and Fleishman (2002, 2004) reported that *A. cristatellus* populations in Puerto Rico occupying closed forest habitats with little light penetration exhibit highly reflective and transmissive dewlaps with more UV reflectance. As light exposure increased (i.e., greater canopy openness), dark dewlaps with low UV reflectance were favored (Leal & Fleishman, 2004).

Several studies on local adaptation of *Anolis* dewlaps have contrasted populations in xeric and mesic habitats. These habitats differ in characteristics such as habitat light, temperature, or precipitation. We sampled brown anole populations across a latitudinal gradient throughout Florida and into southern Georgia. The southeast region of the United States is known to have relatively uniform climatic conditions within seasons. As

624 expected, we found less variation in annual mean temperature and precipitation
625 patterns among our sampled populations (Figure S14b,c) as compared to previous
626 studies of tropical mesic and xeric habitats in Puerto Rico and the Dominican Republic
627 (Leal & Fleishman, 2004, Ng et al., 2013a). Despite this reduced variation in
628 temperature and precipitation, we found that lizards inhabiting cooler environments tend
629 to have dewlaps with greater orange composition, which is consistent with previous
630 studies of *A. distichus* (Ng et al., 2013a). While this may indicate convergent evolution
631 of dewlap orange composition in relation to temperature in *A. distichus* and *A. sagrei*,
632 the underlying mechanism is unknown.
633
634 We found that multiple aspects of the dewlap phenotype are related to invasion history
635 as well as being consistent with natural selection. However, we should not exclude
636 alternative selective pressures that might influence dewlap evolution. Previous studies
637 have proposed the species-recognition hypothesis as a potential explanation for dewlap
638 diversity among sympatric species (Losos, 1985; Vanhooydonck et al., 2009; Baeckens
639 et al., 2018a). This hypothesis predicts that sympatric species will evolve dewlap traits
640 that help distinguish conspecifics from heterospecifics (Rand & Williams, 1970). This
641 possibility has been evaluated within the native range of several anole species (e.g.,
642 Nicholson et al., 2007). However, no study so far has evaluated the role of species
643 recognition in non-native populations. At least seven non-native species of *Anolis*
644 lizards (i.e., *A. cristatellus*, *A. cybotes*, *A. distichus*, *A. equestris*, *A. garmani*, *A.*
645 *porcatus*, and *A. sagrei*) are established in south Florida (Kolbe et al., 2007b). Many of
646 these species have different native ranges, therefore they have not occupied habitats

sympatrically before. To further elucidate the factors that contribute to dewlap diversity among and within species, future studies should evaluate the species-recognition hypothesis in non-native ranges to determine if this pattern persists. Moreover, there might be other unmeasured selective pressures that influence dewlap size in *Anolis* lizards. Previous studies suggest that male brown anole lizards have relatively larger dewlaps when sexual selection (estimated by the degree of sexual size dimorphism) is stronger (Vanhooydonck et al., 2009). Dewlap size may also be determined by intrasexual selection (i.e., male-male competition) since it has been linked to bite force and fighting ability in *Anolis* lizards (Vanhooydonck et al., 2005; Lailvaux & Irschick 2007; Baeckens et al., 2018b). To better understand the evolution of dewlap size in non-native brown anole populations, future studies should consider other potential sources of selection.

In conclusion, the brown anole invasion allowed us to study the evolutionary processes responsible for rapid evolution of an important signaling phenotype during a biological invasion, revealing how both the invasion history and local environments in the non-native range shape among-population variation in dewlaps. Multiple studies reveal the role of genetic admixture in biological invasions (e.g., Kolbe et al. 2007a; Keller & Taylor, 2010) and its association to phenotypic differentiation among non-native populations. Our study further supports the importance of invasion history and admixture in phenotypic evolution and its potential to promote rapid adaptation by increased genetic variation (Kolbe et al., 2004; Keller & Taylor, 2010). Future studies should focus on elucidating the relationship between phenotype and environment in

introduced, as well as native-range, source populations, thus providing specific predictions for phenotypic variation in non-native populations. Lastly, studies should characterize the relative contributions of different evolutionary forces (e.g., admixture, genetic drift, natural selection) to local adaptation and subsequent phenotypic differentiation among non-native populations.

Acknowledgements

We thank Z. Chejanovski for help with fieldwork, as well as J. Breeze, C. Hahn, and M. Gage for help with lizard housing and care at Harvard University. Further, we thank the Genomics and Sequencing Center at the University of Rhode Island for help with constructing the sequencing libraries. This work was supported by the University of Rhode Island and National Science Foundation (NSF) grants (DEB-1354897) awarded to J.J.K., by NSF Graduate Research Fellowship under Grant No. 1747454 to J.N.P.A., by Belgian American Education Foundation (BAEF) to S.B., and by a Natural Sciences and Engineering Research Council of Canada Postdoctoral Fellowship, a Banting Postdoctoral Fellowship, and a Barbour award from the Harvard Museum of Comparative Zoology to D.G.B.

References

Alexander, D. H., Novembre, J., & Lange, K. (2009). Fast model-based estimation of ancestry in unrelated individuals. *Genome Research*, *19*(9), 1655-1664.

Andrade, P., Carneiro, M. (2021). Pterin-based pigmentation in animals. *Biology Letters*, *17*(8), 20210221.

Aulchenko, Y. S., Ripke, S., Isaacs, A., & Van Duijn, C. M. (2007). GenABEL: an R library for genome-wide association analysis. *Bioinformatics*, *23*(10), 1294-1296.

Baeckens, S., Driessens, T., & Van Damme, R. (2018a). The brown anole dewlap revisited: Do predation pressure, sexual selection, and species recognition shape among-population signal diversity? *PeerJ*, 6, e4722.

Baeckens, S., Driessens, T., Huyghe, K., Vanhooydonck, B., Van Damme, R. (2018b). Intraspecific variation in the information content of an ornament: why relative dewlap size signals bite force in some, but not all island populations of *Anolis sagrei*. *Integrative and Comparative Biology*. *58*, 25-37.

Barthel, K. U. (2006). 3D-data representation with ImageJ. *ImageJ Conference*.

Bates, D., Mächler, M., Bolker, B. M., & Walker, S. C. (2015). Fitting linear mixed-effects models using lme4. *Journal of Statistical Software*, *67*(1), 1-48.

Beckschäfer, P. (2015). Hemispherical_2.0. *Batch processing hemispherical and canopy photographs with ImageJ, User Manual.*

Bock, D. G., Baeckens, S., Pita-Aquino, J. N., Chejanovski, Z. A., Michaelides, S. N., Muralidhar, P., … & Kolbe, J. J. (2021). Changes in selection pressure can facilitate hybridization during biological invasion in a Cuban lizard. *Proceedings of the National Academy of Sciences*, *118*(42).

Bock, D. G., Caseys, C., Cousens, R. D., Hahn, M. A., Heredia, S. M., Hübner, S., … & Rieseberg, L. H. (2015). What we still don't know about invasion genetics. *Molecular Ecology*, *24*(9), 2277-2297.

Bock, D. G., Kantar, M. B., Caseys, C., Matthey-Doret, R., & Rieseberg, L. H. (2018). Evolution of invasiveness by genetic accommodation. *Nature Ecology & Evolution*, 2(6), 991-999.

Browning, B. L., & Browning, S. R. (2016). Genotype imputation with millions of reference samples. *American Journal of Human Genetics*, *98*(1), 116-126.

Cheng, R., Parker, C. C., Abney, M., & Palmer, A. A. (2013). Practical considerations regarding the use of genotype and pedigree data to model relatedness in the context of genome-wide association studies. *G3: Genes, Genomes, Genetics*, *3*(10), 1861-1867.

Colautti, R. I., Barrett, S. C. H. (2013). Rapid adaptation to climate facilitates range

734 expansion of an invasive plant. *Science*, 342(6156): 364-366.
735 Colautti, R. I., Maron, J., & Barrett, S. C. H. (2009). Common garden comparisons of
736 native and introduced plant populations: Latitudinal clines can obscure evolutionary
737 inferences. Evolutionary Applications, *2*(2), 187-199.
738 Cole, G. L. (2013). Lost in translation: adaptation of mating signals in changing
739 environments. *Springer Science Reviews*, *1*, 25-40.
740 Crews, D. (1975). Effects of different components of male courtship behaviour on
741 environmentally induced ovarian recrudescence and mating preferences in the
742 lizard, Anolis carolinensis. *Animal Behaviour*, *23*, 349-356.
743 Cummings, M. E. (2007). Sensory trade-offs predict signal divergence in surfperch.
744 *Evolution*, *61*(3), 530-545.
745 Cuthill, I. C., Bennett, A. T., Partridge, J. C., & Maier, E. J. (1999). Plumage reflectance
746 and the objective assessment of avian sexual dichromatism. *The American*
747 *Naturalist*, *153*(2), 183-200.
748 De Meyer, J., Donihue, C. M., Scantlebury, D., Ng, J., Glor, R. E., Losos, J. B., &
749 Geneva, A. J. (2019). Protocol for setting up and rearing a successful lizard room.
750 *Anolis Newsletter VII*.
751 Dlugosch, K. M., & Parker, I. M. (2008). Founding events in species invasions: Genetic
752 variation, adaptive evolution, and the role of multiple introductions. *Molecular*
753 *Ecology,* 17(1), 431-449.
754 Driessens, T., Baeckens, S., Balzarolo, M., Vanhooydonck, B., & Huyghe, K. (2017).
755 Climate-related environmental variation in a visual signalling device: the male and
756 female dewlap in Anolis sagrei lizards. *Journal of Evolutionary Biology*, *30*(10),
757 1846-1861.
758 Duggal, P., Gillanders, E. M., Holmes, T. N., & Bailey-Wilson, J. E. (2008). Establishing
759 an adjusted p-value threshold to control the family-wide type 1 error in genome
760 wide association studies. *BMC Genomics*, *9*(1), 1-8.
761 Endler, J. A. (1993). Some general comments on the evolution and design of animal
762 communication systems. *Philosophical Transactions of the Royal Society of*
763 *London. Series B: Biological Sciences*, *340*(1292), 215-225.
764 Endler, J. A. (1990). On the measurement and classification of color in studies of animal
765 color patterns. *Biological Journal of the Linnean Society*, *41*(4), 315-352.
766 Endler, J. A. (1992). Signals, signal conditions, and the direction of evolution. *The*
767 *American Naturalist*, *139*, S125-S153.
768 Evanno, G., Regnaut, S., & Goudet, J. (2005). Detecting the number of clusters of
769 individuals using the software STRUCTURE: A simulation study. *Molecular*
770 *Ecology*, *14*(8), 2611-2620.
771 Ficetola, G. F., Bonin, A., & Miaud, C. (2008). Population genetics reveals origin and
772 number of founders in a biological invasion. *Molecular Ecology*, *17*(3), 773-782.
773 Fleishman, L. J. (1992). The influence of the sensory system and the environment on
774 motion patterns in the visual displays of anoline lizards and other vertebrates. *The*
775 *American Naturalist*, *139*, S36-S61.
776 Fleishman, L. J., Loew, E. R., & Leal, M. (1993). Ultraviolet vision in lizards. *Nature*,
777 *365*(6445), 397-397.
778 Fleishman, L. J., & Persons, M. (2001). The influence of stimulus and background
779 colour on signal visibility in the lizard Anolis cristatellus. *The Journal of*

780 *Experimental Biology*, *204*(9), 1559-1575.
781 Francis, R. M. (2017). pophelper: an R package and web app to analyse and visualize
782 population structure. *Molecular Ecology Resources*, *17*(1), 27-32.
783 Garrison, E., & Marth, G. (2012). Haplotype-based variant detection from short-read
784 sequencing. *arXiv* preprint arXiv:1207.3907.
785 Geneva, A. J., Park, S., Bock, D., Mello, P. de, Sarigol, F., Tollis, M., … & Losos, J. B.
786 (2021). Chromosome-scale genome assembly of the brown anole (Anolis sagrei), a
787 model species for evolution and ecology. *bioRxiv*. 2021.09.28.462146; doi:
788 https://doi.org/10.1101/2021.09.28.462146.
789 Hijmans, R. J., Cameron, S. E., Parra, J. L., Jones, P. G., & Jarvis, A. (2005). Very high
790 resolution interpolated climate surfaces for global land areas. *International Journal*
791 *of Climatology: A Journal of the Royal Meteorological Society*, *25*(15), 1965-1978.
792 Hodgins, K. A., Bock, D. G., & Rieseberg, L. H. (2018). Trait evolution in invasive
793 species. *Annual Plant Reviews Online*, 1, 459-496.
794 Huey, R. B. (2000). Rapid evolution of a geographic cline in size in an introduced fly.
795 *Science*, 287(5451), 308-309.
796 Jombart, T., & Ahmed, I. (2011). adegenet 1.3-1: new tools for the analysis of genome-
797 wide SNP data. *Bioinformatics*, *27*(21), 3070-3071.
798 Kassambara, A. (2019). ggcorrplot: Visualization of a correlation matrix using 'ggplot2'.
799 *R package version 0.1, 3.*
800 Keller, S. R., & Taylor, D. R. (2008). History, chance and adaptation during biological
801 invasion: Separating stochastic phenotypic evolution from response to selection. In
802 *Ecology Letters*, *11*(8), 852-866.
803 Keller, S. R., & Taylor, D. R. (2010). Genomic admixture increases fitness during a
804 biological invasion. *Journal of Evolutionary Biology*, *23*(8), 1720-1731.
805 Kolbe, J. J., Glor, R. E., Schettino, L. R., Lara, A. C., Larson, A., & Losos, J. B. (2004).
806 Genetic variation increases during biological invasion by a Cuban lizard. *Nature*,
807 *431*(7005), 177-181.
808 Kolbe, J. J., Larson, A., & Losos, J. B. (2007a). Differential admixture shapes
809 morphological variation among invasive populations of the lizard Anolis sagrei.
810 *Molecular Ecology*, *16*(8), 1579-1591.
811 Kolbe, J. J., Glor, R. E., Schettino, L. R., Lara, A. C., Larson, A., & Losos, J. B. (2007b).
812 Multiple sources, admixture, and genetic variation in introduced *Anolis* lizard
813 populations. *Conservation Biology*, 21(6), 1612-1625.
814 Kolbe, J. J., Larson, A., Losos, J. B., & de Queiroz, K. (2008). Admixture determines
815 genetic diversity and population differentiation in the biological invasion of a lizard
816 species. *Biology Letters*, *4*(4), 434-437.
817 Kuznetsova, A., Brockhoff, P. B., & Christensen, R. H. B. (2017). lmerTest Package:
818 Tests in Linear Mixed Effects Models. *Journal of Statistical Software*, *82*, 1-26.
819 Lailvaux, S. P., & Irschick, D. J. (2007). The evolution of performance- based male
820 fighting ability in Caribbean *Anolis* lizards. *American Naturalist*, 170(4), 573-586.
821 Lawson Handley, L. J., Estoup, A., Evans, D. M., Thomas, C. E., Lombaert, E., Facon,
822 … & Roy, H. E. (2011). Ecological genetics of invasive alien species. *BioControl*,
823 *56*(4), 409-428.
824 Leal, M., & Fleishman, L. J. (2002). Evidence for habitat partitioning based on
825 adaptation to environmental light in a pair of sympatric lizard species. *Proceedings*

826 *of the Royal Society. Series B: Biological Sciences*, *269*(1489), 351-359.
827 Leal, M., & Rodríguez-Robles, J. A. (1995). Antipredator responses of Anolis cristatellus
828 (Sauria, Polychrotidae). *Copeia*, 155-161.
829 Leal, M., & Fleishman, L. J. (2004). Differences in visual signal design and detectability
830 between allopatric populations of Anolis lizards. *The American Naturalist*, *163*(1),
831 26-39.
832 Leal, M., & Rodríguez-Robles, J. A. (1997a). Antipredator responses of the Puerto
833 Rican giant anole, Anolis cuvieri (Squamata: Polychrotidae). *Biotropica*, *29*, 372-
834 375.
835 Leal, M., & Rodríguez-Robles, J. A. (1997b). Signalling displays during predator-prey
836 interactions in a Puerto Rican anole, Anolis cristatellus. *Animal Behaviour*, *54*(5),
837 1147-1154.
838 Lee, C. E. (2002). Evolutionary genetics of invasive species. *Trends in Ecology and*
839 *Evolution*, *17*(8), 386-391.
840 Lee, J. C. (1992). Anolis sagrei in Florida: Phenetics of a Colonizing Species III. West
841 Indian and Middle American Comparisons. *Copeia*, *4*, 942-954.
842 Losos, J. B. (1985). An experimental demonstration of the species-recognition role of
843 *Anolis* dewlap color. *Copeia*, 905-910.
844 Losos, J. B. (2009). *Lizards in an Evolutionary Tree: Ecology and Adaptive Radiation of*
845 *anoles*. University of California Press.
846 Lucek, K., Roy, D., Bezault, E., Sivasundar, A., & Seehausen, O. (2010). Hybridization
847 between distant lineages increases adaptive variation during a biological invasion:
848 Stickleback in Switzerland. *Molecular Ecology*, 19, 3995-4011.
849 Macedonia, J. M., James, S., Wittle, L. W. & Clark, D. W. (2000). Skin pigments and
850 coloration in the Jamaican radiation of *Anolis* lizards. *Journal of Herpetology*, 34,
851 99-109.
852 Maia, R., Eliason, C. M., Bitton, P. P., Doucet, S. M., & Shawkey, M. D. (2013). pavo:
853 An R package for the analysis, visualization and organization of spectral data.
854 *Methods in Ecology and Evolution*, *4*(10), 906-913.
855 McLean, C. A., Lutz, A., Rankin, K. J., Stuart-Fox, D., & Moussalli, A. (2017). Revealing
856 the biochemical and genetic basis of color variation in a polymorphic
857 lizard. *Molecular Biology and Evolution*, *34*(8), 1924-1935.
858 Narasimhan, V., Danecek, P., Scally, A., Xue, Y., Tyler-Smith, C., & Durbin, R. (2016).
859 BCFtools/RoH: A hidden Markov model approach for detecting autozygosity from
860 next-generation sequencing data. *Bioinformatics*, 32(11), 1749-1751.
861 Ng, J., Landeen, E. L., Logsdon, R. M., & Glor, R. E. (2013a). Correlation between
862 anolis lizard dewlap phenotype and environmental variation indicates adaptive
863 divergence of a signal important to sexual selection and species recognition.
864 *Evolution*, *67*(2), 573-582.
865 Ng, J., Kelly, A. L., MacGuigan, D. J., & Glor, R. E. (2013b). The role of heritable and
866 dietary factors in the sexual signal of a Hispaniolan *Anolis* lizard, *Anolis distichus*.
867 *The Journal of Heredity*, 104(6), 862-873.
868 Nicholson, K. E., Harmon, L. J., & Losos, J. B. (2007). Evolution of Anolis lizard dewlap
869 diversity. *PLoS one*, *2*(3), e274.
870 Ortiz, E., 1962. Drosopterins in the dewlap of some anoline lizards. *American Zoologist*,
871 *2*(4), 545-546.

Peischl, S., Dupanloup, I., Kirkpatrick, M., & Excoffier, L. (2013). On the accumulation of deleterious mutations during range expansions. *Molecular Ecology*, 22(24), 5972-5982.

Pritchard, J. K., Stephens, M., & Donnelly, P. (2000). Inference of population structure using multilocus genotype data. *Genetics*, *155*, 945-959.

Purcell, S., Neale, B., Todd-Brown, K., Thomas, L., Ferreira, M. A. R., Bender, D., … & Sham, P. C. (2007). PLINK: a tool set for whole-genome association and population-based linkage analyses. *American Journal of Human Genetics*, *81*(3), 559-575.

Puritz, J. B., Hollenbeck, C. M., & Gold, J. R. (2014). dDocent: A RADseq, variant-calling pipeline designed for population genomics of non-model organisms. *PeerJ*, 2, e431.

R Development Core Team, R. (2011). R: a language and environment for statistical computing. *R Foundation for Statistical Computing*.

Rand, A. S., & Williams, E. E. (1970). An estimation of redundancy and information content of anole dewlaps. *The American Naturalist*, *104*(935), 99-103.

Rasband, W. (2012). ImageJ. U. S. National Institutes of Health, Bethesda, Maryland, USA, *http://imagej.nih.gov/ij/*.

Rius, M., & Darling, J. A. (2014). How important is intraspecific genetic admixture to the success of colonising populations? In *Trends in Ecology and Evolution*, *29*(4), 233-242.

Sakai, A. K., Allendorf, F. W., Holt, J. S., Lodge, D. M., Molofsky, J., With, K. A., … & Weller, S. G. (2001). The population biology of invasive species. *Annual Review of Ecology and Systematics*, *32*(1), 305-332.

Sax, D.F., Stachowicz, J.J., Brown, J.H., Bruno, J.F., Dawson, M.N., Gaines, S.D., Grosberg, R.K., Hastings, A., Holt, R.D., Mayfield, M.M., O'Connor, M.I. & Rice, W.R. (2007). Ecological and evolutionary insights from species invasions. *Trends in Ecology and Evolution*, 22(9), 465-471.

Shine, R. (2011). Invasive species as drivers of evolutionary change: cane toads in tropical Australia. *Evolutionary Applications*, *5*(2), 107-116.

Skotte, L., Jørsboe, E., Korneliussen, T. S., Moltke, I., & Albrechtsen, A. (2019). Ancestry-specific association mapping in admixed populations. *Genetic Epidemiology*, *43*(5), 506-521.

Steffen, J.E., & McGraw, K.J. (2007). Contributions of pterin and carotenoid pigments to dewlap coloration in two anole species. *Comparative Biochemistry and Physiology, Part B*, 146: 42-46.

Steffen, J. E., & McGraw, K. J. (2009). How dewlap color reflects its carotenoid and pterin content in male and female brown anoles (*Norops sagrei*). *Comparative Biochemistry and Physiology – B Biochemistry and Molecular Biology*, 154, 334-340.

Stoffel, M. A., Nakagawa, S., & Schielzeth, H. (2017), rptR: repeatability estimation and variance decomposition by generalized linear mixed-effects models. *Methods Ecology and Evolution*, *8*(11), 1639-1644.

Toews, D. P. L., Hofmeister, N. R., & Taylor, S. A. (2017). The evolution and genetics of carotenoid processing in animals. *Trends in Genetics*, *33*(3), 171-182.

Van Belleghem, S. M., Papa, R., Ortiz-Zuazaga, H., Hendrickx, F., Jiggins, C. D., Owen

McMillan, W., & Counterman, B. A. (2018). patternize: An R package for quantifying colour pattern variation. *Methods in Ecology and Evolution*, *9*(2), 390-398.
Vanhooydonck, B., Herrel, A., Meyers, J. J., & Irschick, D. J. (2009). What determines dewlap diversity in Anolis lizards? An among-island comparison. *Journal of Evolutionary Biology*, *22*(2), 293-305.
Vanhooydonck, B., Herrel, A. Y., Van Damme, R., & Irschick, D. J. (2005). Does dewlap size predict male bite performance in Jamaican *Anolis* lizards? *Functional Ecology*, 19(1), 38-42.
Williams, E. E. (1974). Williams Report. *The Second Anolis Newsletter*, 1-10.
Zhou, X., & Stephens, M. (2012). Genome-wide efficient mixed-model analysis for association studies. *Nature Genetics*, *44*(7), 821-824.
Zhu, B. R., Barrett, S. C. H., Zhang, D. Y., & Liao, W. J. (2017). Invasion genetics of Senecio vulgaris: loss of genetic diversity characterizes the invasion of a selfing annual, despite multiple introductions. *Biological Invasions 19*(1), 255-267.

Data Accessibility

Raw sequence data used for this project are available in the Sequence Read Archive (SRA) https://www.ncbi.nlm.nih.gov/sra (BioProject accession PRJNA737437). The scripts used for analyses, the dewlap trait data, the ancestry data, and the environmental data will be made publicly available on Dryad after manuscript acceptance.

Author contributions

J.N.P.A., D.G.B., and J.J.K. designed research; J.N.P.A., D.G.B., and S.B. performed research; J.N.P.A. and D.G.B. analyzed data; and J.N.P.A., D.G.B., S.B., J.B.L., and J.J.K. contributed to writing the paper.

Tables and Figures (with captions)

Tables

Table 1. Results of the linear mixed effects models performed to detect relationships between dewlap traits, Western Cuban ancestry, and environmental variables. Colorimetric variables (i.e., UV reflectance and total brightness) were obtained using edge (P1/P2) and center (P3) dewlap measurements. We log-transformed UV reflectance, total brightness, color composition (i.e., red, orange, yellow) and dewlap area to improve normality. Residual area represents body size-corrected dewlap size. Hue (cut-on wavelength) was inconclusive due to lack of model convergence. Significant P-values are indicated with an asterisk (*).

Dewlap characteristic	Variable	Estimate	Std. Error	DF	T-Statistic	P-value
P1–P3: Total reflectance (PC1)	Intercept	14.333	12.189	27.142	1.176	0.250
	Western Cuban ancestry	11.775	1.700	43.563	6.940	<0.0001 *
	Canopy openness	-0.226	0.065	28.476	-3.457	0.002 *
	Temperature	-0.269	0.410	26.891	-0.655	0.518
	Precipitation	-0.007	0.008	25.309	-0.850	0.403
P1–P3: Total reflectance (PC2)	Intercept	-11.150	8.284	26.960	-1.346	0.189
	Western Cuban ancestry	4.869	1.038	70.350	4.690	<0.0001 *
	Canopy openness	0.037	0.044	26.750	0.835	0.411
	Temperature	0.403	0.279	27.530	1.445	0.160
	Precipitation	-0.001	0.005	25.070	-0.152	0.880
P1 – UV reflectance	Intercept	-2.648	0.513	25.884	-5.161	<0.0001 *
	Western Cuban ancestry	-0.205	0.066	62.479	-3.132	0.003 *
	Canopy openness	0.005	0.003	25.834	1.877	0.072
	Temperature	0.0194	0.017	26.341	1.123	0.272
	Precipitation	0.001	0.001	24.070	1.544	0.136
P2 – UV reflectance	Intercept	-2.073	0.373	26.462	-5.561	<0.0001 *
	Western Cuban ancestry	-0.118	0.052	39.104	-2.252	0.030 *
	Canopy openness	0.008	0.002	26.972	3.840	<0.001 *
	Temperature	-0.009	0.013	25.115	-0.749	0.461
	Precipitation	0.001	0.001	23.749	2.260	0.033 *
P3 – UV reflectance	Intercept	-2.196	0.369	24.108	-5.955	<0.0001 *
	Western Cuban ancestry	-0.126	0.052	37.898	-2.448	0.019 *
	Canopy openness	0.005	0.002	25.423	2.437	0.022 *
	Temperature	0.016	0.012	23.829	1.320	0.199
	Precipitation	0.001	0.001	22.477	0.938	0.358
P1 – Total brightness	Intercept	4.285	0.195	26.620	21.988	<0.0001 *
	Western Cuban ancestry	0.047	0.026	50.290	1.792	0.079
	Canopy openness	-0.004	0.001	27.220	-4.109	<0.001 *
	Temperature	-0.003	0.006	26.710	-0.498	0.622

	Precipitation	9.1e-06	1.2e-04	24.780	0.074	0.942
P2 – Total brightness	Intercept	4.263	0.141	27.980	30.239	<0.0001 *
	Western Cuban ancestry	0.124	0.020	42.810	6.282	<0.0001 *
	Canopy openness	-0.002	0.001	29.640	-2.370	0.025 *
	Temperature	-0.004	0.005	27.600	-0.761	0.453
	Precipitation	-1.5e-04	8.8e-05	26.110	-1.737	0.094
P3 – Total brightness	Intercept	4.299	0.160	26.338	26.950	<0.0001 *
	Western Cuban ancestry	0.100	0.022	40.295	4.456	<0.0001 *
	Canopy openness	-0.002	0.001	27.915	-2.029	0.052
	Temperature	-0.010	0.005	25.972	-1.910	0.067
	Precipitation	-4.1e-05	1.0e-04	24.570	-0.410	0.686
Color composition: Red	Intercept	1.565	39.386	26.201	0.040	0.969
	Western Cuban ancestry	8.731	4.848	73.806	1.801	0.076
	Canopy openness	0.087	0.211	25.859	0.413	0.683
	Temperature	2.209	1.324	26.803	1.669	0.107
	Precipitation	-0.008	0.025	24.402	-0.321	0.751
Color composition: Orange	Intercept	4.739	0.696	26.017	6.805	<0.0001 *
	Western Cuban ancestry	-0.149	0.090	59.048	-1.652	0.104
	Canopy openness	-0.005	0.004	26.050	-1.327	0.196
	Temperature	-0.048	0.023	26.364	-2.028	0.053
	Precipitation	1.7e-04	4.4e-04	24.230	0.393	0.698
Color composition: Yellow	Intercept	1.953	1.253	26.673	1.559	0.131
	Western Cuban ancestry	-0.390	0.152	79.058	-2.588	0.012 *
	Canopy openness	0.006	0.007	26.256	0.846	0.405
	Temperature	-0.029	0.042	27.334	-0.696	0.492
	Precipitation	6.4e-04	8.0e-04	24.849	0.805	0.428
Area	Intercept	0.383	0.155	26.350	2.466	0.021 *
	Western Cuban ancestry	0.075	0.020	63.040	3.787	<0.001 *
	Canopy openness	-0.002	0.001	26.220	-2.320	0.028 *
	Temperature	-0.009	0.005	26.670	-1.677	0.105
	Precipitation	-0.001	0.001	24.500	-1.382	0.180
Perimeter	Intercept	0.182	0.075	25.990	2.411	0.023 *
	Western Cuban ancestry	0.039	0.009	67.050	4.071	<0.001 *
	Canopy openness	-0.001	0.001	25.730	-2.801	0.010 *
	Temperature	-0.003	0.003	26.410	-1.312	0.201
	Precipitation	-0.001	0.001	24.170	-1.567	0.130

953

Table 2. Results of the binomial logistic regression model performed to detect relationships between dewlap pattern, Western Cuban ancestry, and environmental variables (i.e., temperature, precipitation, and canopy openness). We categorized dewlap patterns into two types; 'solid' dewlaps are uniformly colored and may contain a margin and 'spotted' dewlaps having yellowish spots scattered across the reddish center and may also contain a yellow outer margin. Significant P-values are indicated with an asterisk (*).

Variable	Estimate	Std. Error	Z-value	P-value
Intercept	3.249	2.240	1.450	0.147
Western Cuban ancestry	-0.803	0.323	-2.485	0.013 *
Canopy openness	-0.018	0.012	-1.489	0.136
Temperature	-0.014	0.074	-0.197	0.844
Precipitation	-0.002	0.001	-1.293	0.196

Figures

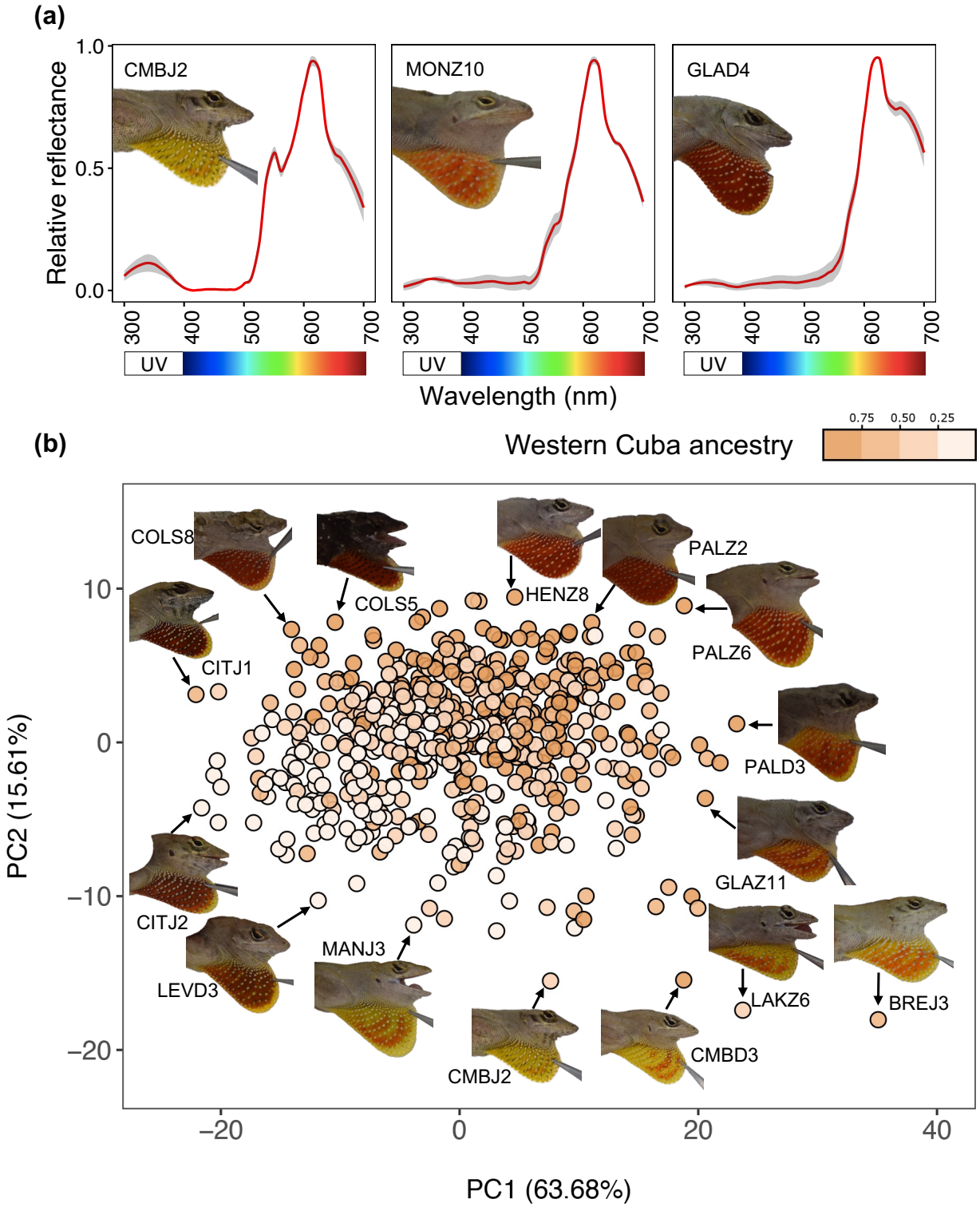

Figure 1. (a) Mean and standard deviation of three representative dewlap phenotypes. The area under the curve of each spectrum was normalized to one prior to averaging. Representative dewlap spectra per population can be found in Figure S3. (b) Results of a PCA for dewlap reflectance for all individuals. Spectral data for each dewlap position (P1, P2, P3)

were included as separate variables divided into 10-nm intervals, resulting in 123 variables. Photos of lizards with their dewlaps extended represent the color variation along each PC axis. High values of PC1 correspond to relatively bright dewlaps, whereas low PC1 values correspond to dull dewlaps. As for PC2, high values correspond to red dewlaps and low values correspond to yellow ones. Shading of points corresponds to the proportion of Western Cuba ancestry inferred from the *K* = 2 STRUCTURE results (see Figure S4).

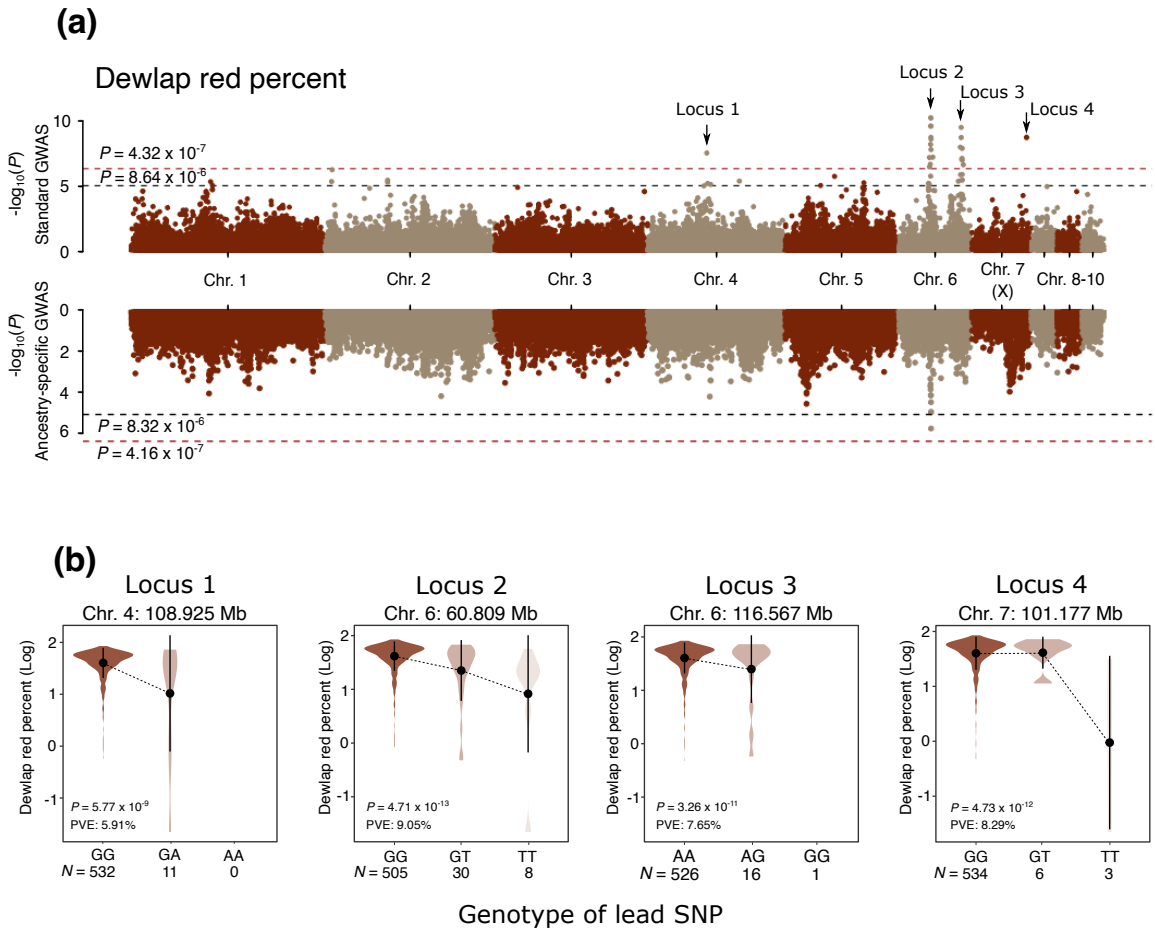

Figure 2. Genome-wide association results for dewlap red color percent. (a) Manhattan plots for the LMM implemented in GEMMA (top) and the ancestry-specific association model implemented in asaMap (bottom), shown for chromosomes 1-10. The red dashed line marks the genome-wide significance threshold calculated using the Bonferroni method. A more permissive suggestive significance level is shown using the black dashed line. Arrows point to the four loci associated with the focal trait. (b) Dewlap red percent (log-transformed) values shown for each genotype at the four significant loci. Note that genotype GG at locus 3 is not shown due to limited sample size available (N = 1). For each genotype class, points show the mean, and the black lines indicate standard deviation. Association results for all traits are shown in Figure S12.

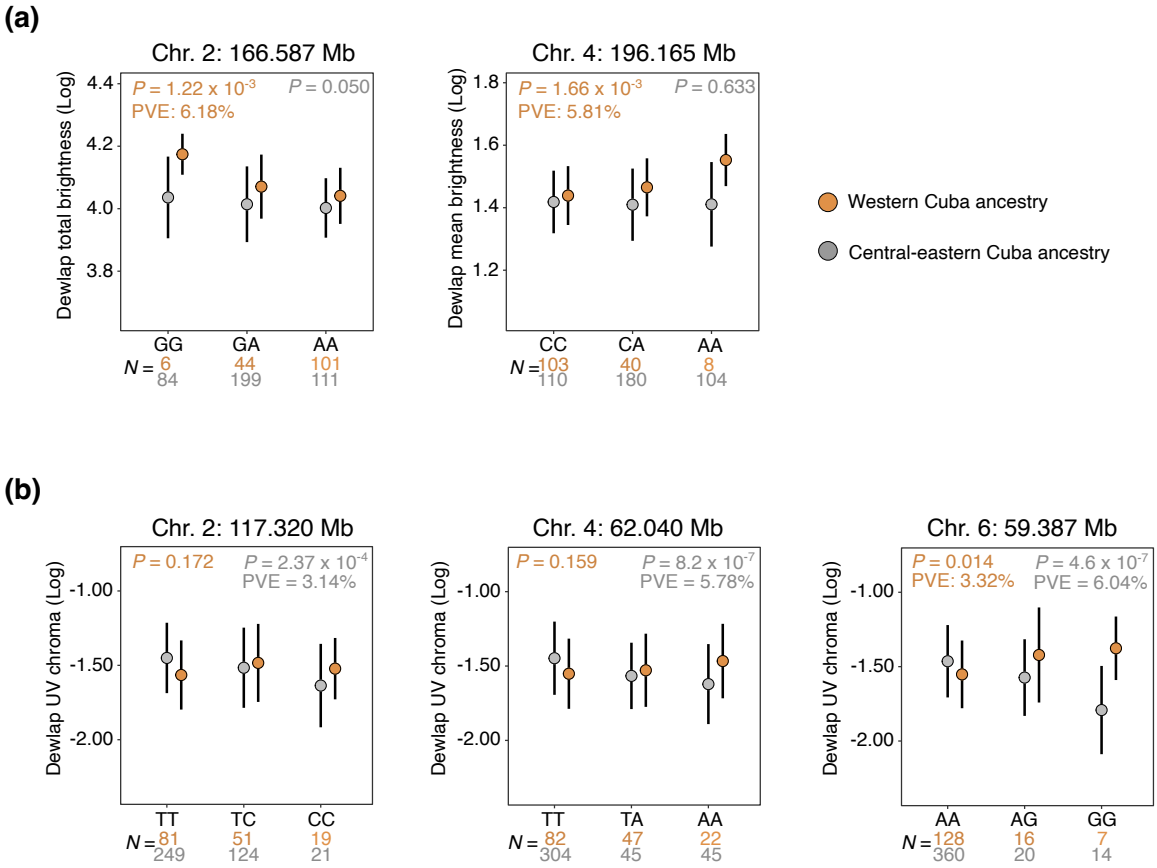

Figure 3. Ancestry-specific associations identified for dewlap brightness (a) and for dewlap UV chroma (b). The effect of alleles at each SNP on trait values was calculated separately for the "Western Cuba ancestry" and the "Central-eastern Cuba ancestry" sample groups (sample sizes for each sample group are given below each genotype).